Self-Assembly of Solid Polyelectrolyte−Silicon−Surfactant Complexes

ARTICLE *in* LANGMUIR · SEPTEMBER 1998

Impact Factor: 4.46 · DOI: 10.1021/la980229g

Self-Assembly of Solid Polyelectrolyte−Silicon−Surfactant Complexes

Andreas F. Thünemann* and Kai Helmut Lochhaas

Max Planck Institute of Colloids & Interfaces, Kantstrasse 55, D-14513 Teltow-Seehof, Germany

Received February 24, 1998. In Final Form: July 20, 1998

Two solid complexes of surfactants with a pendant trimethylsilyl moiety and a cationic polyelectrolyte are prepared. These complexes form smectic A-like lamellar mesophases and low-energy surfaces (20 and 36 mN/m). The lamellar structures are characterized in detail by small-angle X-ray scattering using the interface distribution function concept. Both complexes are fabricated as highly transparent, flexible films with tensile moduli of 12 and 30 MPa and low glass transition temperatures (−10 and −56 °C). The application of the complexes as new coating materials is discussed.

1. Introduction

Many silicones have outstanding surface-modifying properties, e.g., the ability to reduce surface energy, which are responsible for many of their applications. The origins of the unusual and useful surface properties are closely related to the silicones' unique chemistry.[1] Silicon-containing surfactants have been successfully used as auxiliaries in the manufacturing and processing of paints and coatings.[2,3] They are also valuable as surface-active ingredients in the textile and fiber industries, acting as emulsifiers, softeners, etc.[4] The aggregation behavior of silicon-containing surfactants has been investigated in detail by small-angle neutron and static light scattering, where, for example, hexagonal and lamellar mesophases were found in concentrated aqueous solution.[5] Nothing has yet been reported on the formation of ordered structures, on a nanometer scale, in solid complexes of polyelectrolytes and silicon surfactants. Comparable complexes of fluorine-containing surfactants and polyelectrolytes, which form ultralow-energy surfaces with a surface tension clearly below 20 mN/m, have already been described.[6] Such complexes are very promising as coating materials, but the use of fluorine complexes is limited due to the extremely high prices of fluorine surfactants. Therefore, for water-repellent applications, it is desirable to substitute the fluorine surfactants with silicon surfactants.

In this work we report the preparation and properties of complexes **3a** and **3b**, formed using a cationic polyelectrolyte, poly(dimethyldiallylammonium chloride) (**1**), and the anionic surfactants isopropylammonium 6-(trimethylsilyl)-*n*-hexylsulfate (**2a**) and isopropylammonium [3-(1,1,3,3,5,5,5-heptamethyltrisiloxan-1-yl)hexyl-1-sulfate] (**2b**). The complex formation is shown schematically in Figure 1. Polyelectrolyte **1** was chosen because it has already been used successfully for many different solid complexes, e.g., with lipids,[7] amphipilic drugs,[8] and fluorinated surfactants. The silicon surfactant **2**, with only one trimethylsilyl moiety, was chosen for different

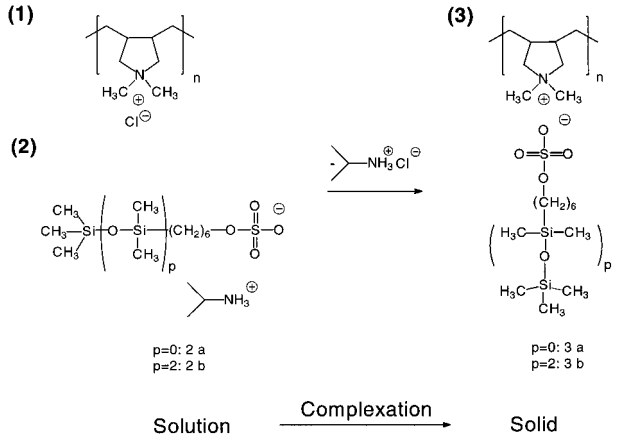

Figure 1. Sketch of complex formation: (1) poly(diallyldimethylammonium chloride); (2) isopropylammonium 6-(trimethylsilyl)-*n*-hexylsulfate (p = 0, **2a**) isopropylammonium [3-(1,1,3,3,5,5,5-heptamethyltrisiloxan-1-yl) and hexyl-1-sulfate] (*p* = 2, **2b**); (3) stoichiometric polyelectrolyte−surfactant complex.

reasons: First, salts of sulfatic esters have excellent surfactant properties combined with good hydrolysis stability,[9] and second, it is known that the chemical and physical behavior of silicon compounds, e.g., their high flexibility, is very different from that of their carbon analogues. It must be expected that our experience with non-silyl-containing complexes can only be transferred to silicon-containing surfactants if the influence of silicon is not predominate. Additionally, only atoms at, or nearby, the film/air interface are responsible for the surface energy. A perfect alignment of $(CH_3)_3Si$ groups at the film surface should result in a surface energy significantly lower than that found for high molecular weight poly(dimethylsiloxane) (24 mN/m).[1] In principle, one trimethylsilyl moiety at the tail of the surfactant may be enough to form a low-energy surface material. For example, sodium methylsiliconate $(CH_3Si(OH)_2ONa)$ is used successfully in the hydrophobation of walls while maintaining permeability for moisture.[10] The trisiloxanylhexamethylsulfate **2b** was

(1) Owen, M. J. *Ind. Eng. Chem. Prod. Res. Dev.* **1980**, *19*, 97−103.
(2) Fink, H. F. *Tenside, Surfactants, Deterg.* **1991**, *28*, 306−312.
(3) Dams, R. *Tenside, Surfactants, Deterg.* **1993**, *30*, 326−327.
(4) Schmidt, G. *Tenside, Surfactants, Deterg.* **1990**, *27*, 324−328.
(5) Gradzielski, M.; Hoffmann, H.; Robisch, P.; Ulbricht, W.; Grüning, B. *Tenside, Surfactants, Deterg.* **1990**, *27*, 366−379.
(6) Antonietti, M.; Henke, S.; Th ünemann, A. *Adv. Mater.* **1996**, *8*, 41−45.
(7) Antonietti, M.; Kaul, A.; Thünemann, A. *Langmuir* **1995**, *11*, 2633−2638.
(8) Thünemann, A. *Langmuir* **1997**, *13*, 6040−6046.
(9) Klein, K. D.; Schaefer, D.; Lersch, P. *Tenside, Surfactants, Deterg.* **1994**, *31*, 115−119.

S0743-7463(98)00229-7 CCC: $15.00
Published on Web 09/15/1998

synthesized in order to compare the influence of a single silyl group **2a** with a trisiloxane on the structure and surface energy of equivalent complexes. To the best of our knowledge, the substance isopropylammonium [3-(1,1,3,3,5,5,5-heptamethyltrisiloxan-1-yl)hexyl-1-sulfate] is not documented in the literature.

2. Experimental Section

A. Materials. High molecular weight poly(diallyldimethylammonium chloride) (PDADMAC; 20% w/w aqueous solution) was purchased from Aldrich Chemical Co. and used as received. The molecular weight of PDADMAC was determined by viscosimetry in a 0.5 M NaCl solution to be on the order of $M_v = 180\,000$. The result of aqueous gel permeation chromatography (GPC) was $M_v = 623\,000$, and $M_v = 180\,000$ (0.5 mol/dm^3 $NaNO_3$, Progel-TSK-PW column by Tosohaas, refraction index and light scattering detector). The solvent for film casting was high-performance liquid chromatography (HPLC)-grade ethanol (Aldrich Chemical Co.). Isopropylammonium 6-(trimethylsilyl)-*n*-hexylsulfate was purchased from Th. Goldschmidt AG and used as received. According to a route described elsewhere[11] [3-(1,1,3,3,5,5,5-heptamethyltrisiloxan-1-yl)hexyl-1-sulfate] can be easily obtained in three steps. (i) Trimethylsilyl 5-hexen-1-yl ether: 19 g (189.7 mmol) of 5-hexen-1-ol and 30 g (186.3 mmol) of hexamethyldisilazane were heated under reflux for 24 h in an argon atmosphere. A further quantity of 15 g (93.15 mmol) of hexamethyldisilazane was then added. The product was purified via vacuum distillation at 10 mbar and 60 °C. (ii) [3-(1,1,3,3,5,5,5-heptamethyltrisiloxan-1-yl)hexyl trimethylsilyl ether: 22.5 g (101.4 mmol) 1,1,3,3,5,5,5-heptamethyltrisiloxane was reacted with 15.87 g (92.2 mmol) of trimethylsilyl 5-hexen-1-yl ether using 0.1 g of Lamoreaux catalyst.[12] The reaction mixture was kept at 100 °C for 1.5 h, followed by an additional 1.5 h at 140 °C with stirring. The end of the reaction was characterized when refluxing of the heptamethyltrisiloxane was no longer observed. The ether group was then cleaved by adding 26.91 g of ethanol and 1.17 g of water at 80 °C. The resulting (1,1,3,3,5,5,5-heptamethyltrisiloxan-1-yl)hexan-1-ol was purified by vacuum distillation (118 °C at 2.7 mbar). (iii) [3-(1,1,3,3,5,5,5-heptamethyltrisiloxan-1-yl)-hexyl-1-sulfate] was synthesized by adding 3.8 g (39.2 mmol) of amidosulfonic acid to a solution of 3.0 g (41.1 mmol) of *N*,*N*-dimethylformamide and 12 g (37.3 mmol) of (1,1,3,3,5,5,5-heptamethyltrisiloxan-1-yl)hexan-1-ol. After the starting materials were dissolved, the mixture was heated to 75 °C within 0.5 h and kept at that temperature for 5 h. A total of 2.4 g of 2-propanol was added to the resulting material. The excess amidosulfonic acid was filtered while hot, and residues of acid were neutralized using isopropylamine. The product was purified by distillation at 2.5 mbar (80 °C). The yield was 16 g (20.1% with respect to 5-hexan-1-ol).[13] C NMR in DMSO-d_6: δ (ppm) 0−3 (C7−C13), 18 (C6), 23 (C5), 25 (C4), 29 (C3), 33 (C2), 63 (C1).

$$O_3SOCH_2\,(1)-CH_2\,(2)-CH_2\,(3)-CH_2\,(4)-CH_2\,(5)-CH_2\,(6)-Si(CH_3)_2(7,13)-O\,Si(CH_3)_2\,(8,12)-OSi(CH_3)_3\,(9,10,11)$$

B. Complex Formation. A total of 5 g (16 mmol) of isopropylammonium 6-(trimethylsilyl)-*n*-hexylsulfate was dissolved in 100 mL of distilled water and adjusted to pH 8 using dilute NH_3. The mixture was stirred with an ultraturrax at 9500 rad/min, while 24.6 g of an aqueous PDADMAC solution (10% w/w PDADMAC, 15.2 mmol) was added dropwise. The resulting crude complex was filtered off immediately and washed with water. This method produced 5.77 g of complex **3a** (80% theoretical yield). Elemental analysis of the complex showed the chloride content to be lower than 0.1%. Free-standing films of the complex were cast by pouring the solutions onto glass plates. The two-dimensional geometry of the films was controlled by glass frames of variable size which were mounted on top of the glass plate. After evaporation of the solvent at 20 °C, the remaining traces of solvent were removed in vacuo at room temperature for 24 h. Elem anal. for complex **3a**. Obsd (calcd for a 1:1 stoichiometry)]: C, 50.38 (53.79); H, 9.78 (9.82); N, 3.35 (3.69); S, 7.45 (8.45). Elem anal. for complex **3b**. Obsd (calcd for a 1:1 stoichiometry)]: C, 47.30 (47.78); H, 9.63 (9.36); N, 2.40 (2.65); S, 6.29 (6.07).

C. Subsection Methods. Wide-angle X-ray scattering (WAXS) measurements were carried out with a Nonius PDS120 powder diffractometer in transmission geometry at 18 ± 2 °C. A FR590 generator was used as the source for Cu Kα radiation; monochromatization of the primary beam was achieved by means of a curved Ge crystal. The scattered radiation was measured with a CPS120 position-sensitive detector. The resolution of this detector is better than 0.018°. Small-angle X-ray scattering measurements (SAXS) were recorded with a Kratky camera (Anton Paar, Austria) at 18 ± 2 °C. WAXS and SAXS cuves were recorded for films with thicknesses in the range of 0.1−1 mm. Within this range, the scattering curves do not depend on the film thickness. Differential scanning calorimetry (DSC) measurements were performed on a Netzsch DSC 200 (Germany). The samples were examined at a scan rate of 10 K/min in two heating and one cooling scans. The first and second heating traces were essentially identical. Stress−strain measurements were carried out with a Zwick Material-Tester Z010 (Germany). Molecular modeling simulations of the complexes were performed using Insight & Discover (BIOSYM Technologies, USA).

3. Results and Discussion

The complexation of PDADMAC (**1**) with **2a** and **2b** affords the ionic complexes **3a** and **3b** (see Figure 1). The complexes can be processed as transparent and flexible films by solvent-casting or spin-coating. Free-standing films with thicknesses down to 50 μm can be produced by the solvent-casting method without any difficulty. Many silicon-free polyelectrolyte−surfactant complexes are mesomorphical ordered and structurally similar to liquid crystals. Because of their physicochemical relationship to hydrocarbon polyelectrolyte−surfactant complexes, we expect self-organizing behavior for complexes **3a** and **3b**.

A. SAXS. To study the mesomorphic character of the complexes, small-angle X-ray scattering experiments were conducted (powder and films). The resulting scattering curves of **3a** and **3b** are shown in Figure 2. In the scattering curves of both complexes, an intense maximum that confirms the assumption of a microphase-separated system is found. The reflex positions and widths further revealed that complex **3b** has a larger, less ordered structure than **3a**. No reflexes of higher order are present, which does not allow the precise assignment of the phase structure. To obtain this information, a more detailed evaluation of the data has to be carried out. For determining the long period, the smearing effect of the

(10) Falbe, J.; Regitz, M. *Römpp Lexikon Chemie*; Thieme: Stuttgart, 1995.
(11) DE 4141046C1.
(12) U.S. Patent No. 3,220,972.
(13) Ruland, W. Private communication.

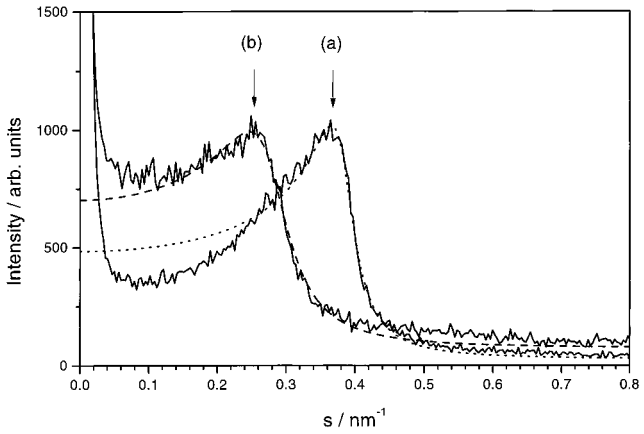

Figure 2. Small-angle X-ray curves of complexes **3a** and **3b** and fits according to eq. 4.2.

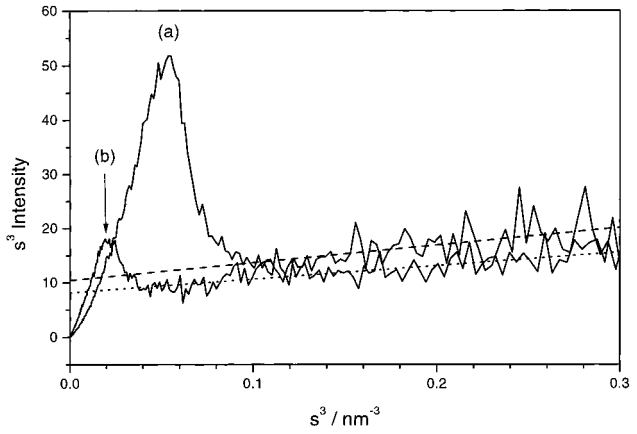

Figure 3. s^3J-s^3 plots of the small-angle X-ray scattering of complexes **3a** and **3b** and the ideal behavior according to Porod's law of **3a** (dashed line) and **3b** (dotted line).

camera system has to be taken into account. The use of a Kratky camera results in a characteristic peak profile due to slit-length smearing of the experimental setup. The broader the peak, the more the peak maximum deviates from the real reflex position, s_h, which would, for example, be measured with a pinhole system. To determine the reflex position and its integral width b, an analytical expression of a slit-smeared, three-dimensional Lorentzian distribution was used:

$$J(s) = \frac{1}{2s_h}\left(\frac{(A^2 + B^2)^{1/2} - A}{2(A^2 + B^2)}\right) \qquad (4.1)$$

with $A = b^2 + \pi^2(s^2 - s_h^2)$ and $B = 2\pi b s_h$. J represents the slit-smeared intensity obtained using a Kratky camera and s_h the reflex position without slit-smearing effects. This expression was fitted to the Kratky peaks' resulting in $d_a = 1/s_a = 2.63$ nm, $d_b = 1/s_b = 3.57$ nm, $b_a = 0.086$ nm^{-1}, and $b_b = 0.140$ nm^{-1} (see Figure 2, where a corresponds to complex **3a** and **b** to complex **3b**). The results obtained from the refined evaluation of the X-ray data were confirmed by molecular modeling calculations. Calculating a lamellar, smectic A-like structure consisting of alternating polyelectrolyte and surfactant layers gave ca. 2.6 nm for **3a** and ca. 3.5 nm for **3b**. From the s_h and b values, it can be assumed that **3a** and **3b** are isomorphous but that **3b** has a larger and less perfect structure than **3a**.

Further information about the structures can be obtained from the asymptotic decrease of the scattering curve. At values in the range of 0.5−0.8 nm^{-1}, the scattered intensity decreases with the third power of the scattering vector. This is in accordance with Porod's law.[14,15] Such a scaling law is a strong indication for a two-phase system with sharp interface boundaries. Porod's law is given by[14]

$$\lim_{s\to\infty} 4\pi^2 s^3 J(s) = k/l_p \qquad (4.2)$$

where the scattering vector is defined by $s = q/2\pi = 2/\lambda \sin(\theta)$, θ is the Bragg angle, λ is the wavelength, J is the slit-smeared scattering intensity, l_p is the average chord length, and k is the invariant.

$$k = 2\pi \int_0^\infty s J(s)\, ds \qquad (4.3)$$

The main source of error in the range of validity of Porod's law is the scattering due to density fluctuations and the width of the domain boundary.[16] The linear behavior of the scattering curve in a $s^3J(s)-s^3$ plot (Figure 3) proves that the only deviation from Porod's law is a three-dimensional homogeneous density fluctuation, which is given by the slope of the straight line. A broader transition or a statistical structuring of the domain boundary, as is typically observed for microphase-separated block copolymers, for example,[17] can be excluded. Small deviations from a sharp boundary would lead to strong and significant deviations from Porod's law.[16] Therefore, we can conclude that the phase boundaries of both complexes are on the order of 1 or 2 atomic distances. Using eq 4.2, the average chord lengths were calculated to be 1.23 nm (complex **3a**) and 1.27 nm (complex **3b**). It should be noted that the values for the average chord length of both complexes are very similar, although the d values are very different. This is indicative of the complexes being microphase-separated, constructed of a smaller ionic phase (polyelectrolyte plus sulfonate headgroups) and a larger nonionic phase (hydrophobic moieties). Regarding the definition of the chord length ($1/l_p = \langle 1/\langle l_1\rangle_n\rangle_w + \langle 1/\langle l_2\rangle_n\rangle_w$),[14,15,18] it becomes clear that the smaller distances are much higher-weighted than the larger. From the similarity of both chord lengths, we can conclude that the ionic phases of **3a** and **3b** are nearly identical.

In the special case of a lamellar two-phase system, the parameter l_p is related to the average thicknesses of the lamellae by $l_p = c_1 l_2 = 2c_1 d_2 = c_2 l_1 = 2c_2 d_1$, where c_1 and c_2 are the volume fractions of the lamellae and d_1 and d_2 are their thicknesses.[18] Consequently, l_p is in the range of $0 \le l_p \le (d_1 + d_2)/2 = L/2$. From experimental analysis the long period of **3a** is 2.63 nm; the maximum value, $l_{p,max}$, theoretically is 1.32 nm. Other mesophases show smaller maximum values of l_p. Therefore, although no higher order reflexes can be observed in the small-angle scattering curve, a lamellar mesophase structure and flat lamellar surfaces can be assumed to be very likely for complex **3a**. This is different from the highly undulated lamellae found for polyelectrolyte−lipid complexes reported previously.[7,19] In contrast to complexes with

(14) Porod, G. *Kolloid-Z.* **1951**, *124*, 83−114.
(15) Porod, G. *Kolloid-Z.* **1952**, *125*, 51−122.
(16) Siemann, U.; Ruland, W. *Colloid Polym. Sci.* **1982**, *260*, 999−1010.
(17) Wolff, T.; Burger, C.; Ruland, W. *Macromolecules* **1994**, *27*, 3301−3309.
(18) Ruland, W. *Colloid Polym. Sci.* **1977**, *255*, 417−427.

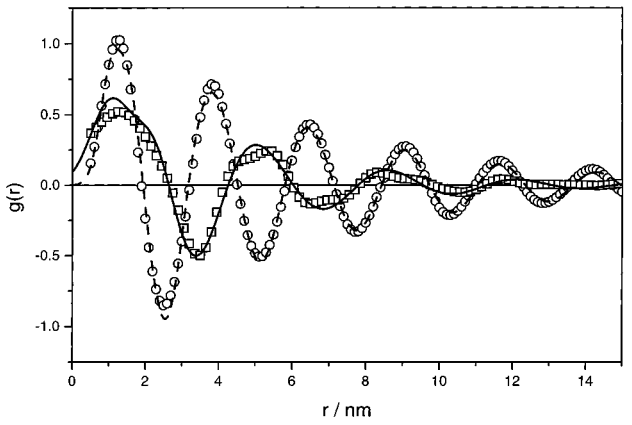

Figure 4. Interface distribution functions computed from the experimental values for complexes **3a** (squares) and **3b** (circles). The solid line is the theoretical curve for complex **3a** with lamellar thicknesses of $d_1 = 1.03$ nm and $d_2 = 1.55$ nm. The dashed line is the theoretical curve for complex **3b** with $d_1 = 1.03$ nm and $d_2 = 2.31$ nm.

undulated surfaces, the silicon surfactant **2a** is monodisperse, has a very short alkyl chain, and, in addition to a bulky headgroup [SO_4^-], also has a large tail group [Si(CH$_3$)$_3$]. The same considerations for **3b** do not allow an unambiguous determination of the mesophase of this complex. The long period of a lamellar system L is given by $L = d_1 + d_2$, where d_1 and d_2 are the thicknesses of the two lamellae. Their values can be determined by calculating the interface distribution function $g(r)$,[18] which is defined by the second derivative of the one-dimensional autocorrelation function for positive definite values of the distance r in real space. The interface distribution function can be computed by a combination of inverse Fourier transformation and slit desmearing:

$$g(r) \propto \int_0^\infty G(s)\left(4J_0(2\pi rs) - \frac{1 - 4\pi^2 r^2 s^2}{\pi rs} J_1(2\pi rs)\right) \mathrm{d}s \tag{4.4}$$

where J_n is the Bessel function of the first kind and nth order. $G(s)$ is the interference function defined by

$$G(s) \propto [\lim_{s\to\infty} s^3 J(s)] - s^3 J(s) \tag{4.5}$$

The interface distribution function can be written in the form[18]

$$g(r) \propto h_1 + h_2 - 2h_{12} + h_{121} + h_{212} - 2h_{1212} + \ldots \tag{4.6}$$

where h_i are normalized distributions of the distances between interfaces measured perpendicular to the planes of the lamellae. A model successfully applied to describe the statistics of lamellar phases is the stacking model in which the statistic is determined by the distributions $h_1(d_1)$ and $h_2(d_2)$ of the lamellar thicknesses.[17] In Figure 4, the interface distribution functions computed from the scattering curves and the best fits using the stacking model are plotted. For complex **3a**, this results in $L = 2.58$ nm, $d_1 = 1.03$ nm, and $d_2 = 1.55$ nm. For complex **3b** the values are $L = 3.34$ nm, $d_1 = 1.03$ nm, and $d_2 = 2.31$ nm. The smaller lamellar type is for both complexes have the same thickness. These 1.03-nm-thick lamellae are formed by polyelectrolyte chains and sulfate groups, which are very likely to be identically structured for both complexes. The 1.55-nm-thick lamellae of **3a** are built of −(CH$_2$)$_6$ Si(CH$_3$)$_3$ groups, and the 2.31-nm-thick lamellae of **3b** are built of −(CH$_3$)$_6$Si(CH$_3$)$_2$OSi(CH$_3$)$_2$OSi(CH$_3$)$_3$ groups.

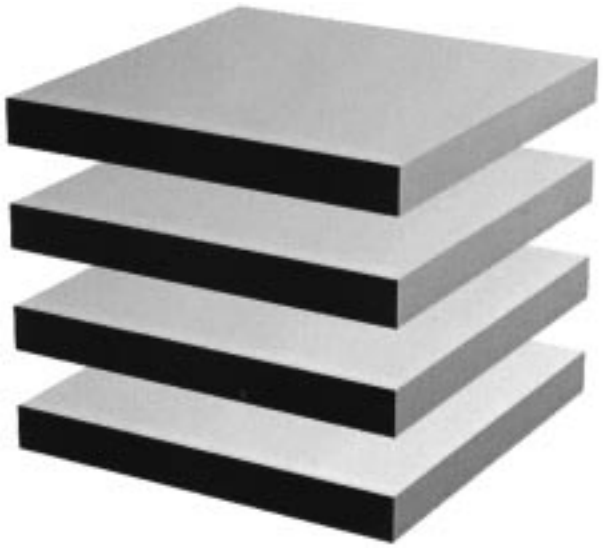

Figure 5. Model of the perforated layer structure. The polyelectrolyte phase is plotted gray, with a thickness of 1.03 nm for both complexes. Surfactant molecules are filling the space between the polyelectrolyte phases (not drawn). The thicknesses of these hydrophobic chain layers are 1.55 and 2.31 nm for **3a** and **3b**, respectively.

In addition to the lamellar thicknesses, the curvature of the interface between ionic and nonionic domains is an important feature for the description of the complex morphology. If the interfaces of the lamellae are completely planar and the lateral dimensions are large compared to the thicknesses of the lamellae, the total interface area per volume is given by $S_0/V = 2/L$. If the interface is not planar, the total interface area S obtained from l_p is larger than S_0 obtained from L. A measure of the planarity of the interfaces is obtained from the ratio

$$\frac{S}{S_0} = \frac{2d_1 d_2}{L l_p} \tag{4.7}$$

Using eq 4.7, a surface ratio of 1.01 is calculated for **3a** and of 1.12 for **3b**. From these values we conclude that the lamellar surfaces of **3a** are perfectly planar (see Figure 5) and those of **3b** show only small undulations. Obviously, the surfaces of these complexes show almost no curvature and, therefore, have a low curvature energy. This finding stands in contrast to those for polyelectrolyte−lipid complexes,[7,19] for example, some of whose lamellar mesophases show high undulations with S/S_0 values up to 1.38. The lipids of the complexes described there have a broad alkyl chain length and headgroup distribution. Further, Antonietti et al.[20] showed that the undulations of poly(styrenesulfonate)−alkyltrimethylammonium surfactant complexes increase with increasing alkyl chain length. We attribute the lack of undulations of complex **3a** to the small hydrophobic chain length and an appropriate charge density of the polyelectrolyte **2a**. The small undulations of **3b** can be explained by packing disorder of the bulky siloxane groups.

(19) Antonietti, M.; Wenzel, A.; Thünemann, A. *Langmuir* **1996**, *12*, 2111−2114.

(20) Antonietti, M.; Conrad, J.; Thünemann, A. *Macromolecules* **1994**, *27*, 6007−6011.

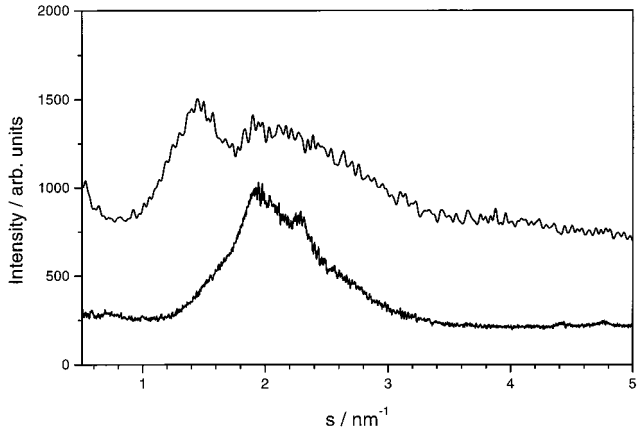

Figure 6. Wide-angle X-ray curves of complexes **3a** (lower curve) and **3b** (upper curve).

B. WAXS. Films of both complexes are flexible and transparent, which indicates that the materials are noncrystalline. To evaluate the state of order on an atomic length scale, wide-angle X-ray scattering measurements on the complex powders and films were conducted. No differences between powder and film curves could be found. The wide-angle X-ray scattering curve of **3a** (see Figure 6) exhibits two broad overlapping maxima around 2.0 and 2.3 nm^{-1}, indicating a liquidlike packing of molecules. The first and more intense maximum corresponds to a Bragg spacing of about 0.52 nm. This value is considerably higher than that observed for the amorphous packing of saturated alkyl chains in complexes of low molecular weight surfactants with synthetic polypeptides (0.45 nm)[21] or that observed for poly(styrenesulfonate)−surfactant complexes (0.43 nm).[20] The lower maximum position, compared with that observed in complexes with longer alkyl chains, indicates that the average atomic distance in the silicon-containing complexes is significantly larger. This is expected due to the high relative amount of the larger atoms silicon and sulfur. These atoms cause a higher average atomic distance than that observed in complexes without silicon. The weaker maximum at 2.3 nm^{-1} corresponds to a Bragg spacing of 0.44 nm, which is a typical value for the packing of alkyl chains in polyelectrolyte−surfactant complexes. In the region of 1.8−3.0 nm^{-1}, where the maxima of complex **3a** were found, the WAXS curve of **3b** (upper curve in Figure 6) shows only a single broad maximum. This indicates an even broader distribution of atomic distances in the polyelectrolyte and hexyl chains of complex **3b** than that of **3a**. In addition to the broad, intense maximum at lower angles, a sharper maximum is found corresponding to a Bragg distance of 0.69 nm. This can be attributed to larger distances due to dimethylsiloxane entities, which have a diameter of about 0.7 nm. As is frequently observed for solid polyelectrolyte−surfactant complexes, the WAXS data of complexes **3a** and **3b** confirm that both are amorphous on an atomic length scale.

C. Surface Characterization. Surface energies of complexes **3a** and **3b** were determined by wettability measurements with different test liquids: water, glycerol, and methylene diiodide. Films of the complexes were solvent-cast onto glass slides. The wettability of the complex films was then determined by dynamic contact angle measurements. For comparison of the contact angle data, the solid surface energies were calculated using an expression derived by Neuman and Li[22]

Table 1. Solid Surface Tensions for Complex Surfaces

liquid	liquid surface tension [mN/m]	complex	contact angle θ [deg]	solid surface tension [mN/m]
water	72.75	**3a**	74 ± 7	39
		3b	105 ± 5	20
glycerol	63.11	**3a**	65 ± 8	38
		3b	94 ± 4	21
methylene diiodide	50.80	**3a**	50 ± 8	36
		3b	79 ± 6	22

$$\cos\theta = -1 + 2\sqrt{\frac{\gamma_{sv}}{\gamma_{lv}}}\exp[-0.00012747(\gamma_{lv} - \gamma_{sv})^2] \quad (4.8)$$

where $\cos\theta$ is the advancing contact angle, γ_{sv} the solid surface tension, and γ_{sv} the liquid surface tension of the used test liquid. Equation 4.8 results in surface energies of 36−39 mN/m for complex **3a** and 20−22 mN/m for complex **3b** (see Table 1). Liquids with low polarity, e.g., decane, are rapidly adsorbed and spread on surfaces of both complexes. The surface energies calculated for **3b** are close to those of dimethylsiloxane surfaces (21−23 mN/m).[1] From the low surface energies and the strong segregation into periodic ionic and nonionic layers derived by SAXS, we conclude that siloxane moieties are mainly located on the surface of complex **3b**. Similar to poly(dimethylsiloxane)s,[1] the surface activity of **3b** approximates that of a relatively closely packed array of methyl groups. The surface energy of **3a** is significantly higher than that of **3b**, comparable, for example, with values reported for poly(ethylene terephthalate) surfaces (35−36 mN/m).[22] We explained that both complexes are well-ordered lamellar structures, but only **3b** forms low-energy surfaces for a number of reasons: Obviously, it is not enough to have intrinsically surface-active pendant groups, but they must also be correctly oriented. It might be that a perfect alignment of trimethylsilyl groups causes problems with a dense packing of methylene groups among silyl and sulfate moieties. Furthermore, the carbon−silicon bond shows a dipole moment with a partially negative charge located at the carbon atom. A perfect alignment of trimethylsilyl groups on the surface results in an energetically unfavorable alignment of the dipole. In contrast to the unfavorable packing conditions of **3a**, the siloxane backbone of **3b** is an extended, flexible chain, with the available methyls adopting the lowest surface energy orientation. It should be stressed here that the surfaces of the complexes **3a** and **3b** show a tendency to swell when in contact with water. This phenomenon is commonly known for poly(dimethylsiloxane) coatings. Only for annealed poly(dimethylsiloxane) was a surface energy of about 24 mN/m found. Without annealing the surface energies are significantly higher.[1] Flexibility of the siloxane chains allows water molecules to penetrate the film. The heat treatment may cross-link molecules in the film, so that the methyl groups cannot reorientate themselves when in contact with water. Therefore, effective silicon water-repellent treatments are cross-linked or reacted onto the fabric. The decomposition of the PDADMAC backbone at higher temperatures makes it impossible to adopt this common heat treatment for the complexes **3a** and **3b**.

(21) Ponomarenko, A.; Waddon, A. J.; Bakeev, K. N.; Tirrell, D. A.; MacKnight, W. J. *Macromolecules* **1996**, *29*, 4340−4345.

(22) Li, D.; Neumann, W. *J. Colloid Interface Sci.* **1991**, *148*, 190.

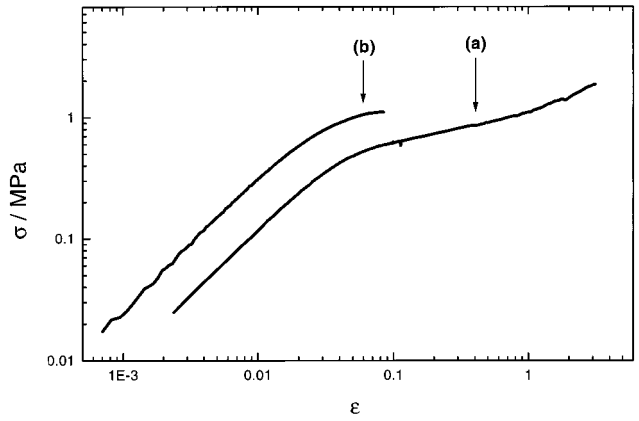

Figure 7. Stress−strain curves of complex **3a** and **3b** films.

D. Mechanical Properties. To quantify the mechanical properties, stress−strain measurements were performed on free-standing films with thicknesses of about 75−80 μm. Stress−strain curves of complex **3a** films (Figure 7) show approximately Hooke's behavior (reversibility and proportionality) up to stress values of 0.4 MPa and a strain of about 4%. The corresponding values for **3b** are 0.8 MPa and 2%. Tensile moduli were determined to be 12 MPa (**3a**) and 30 MPa (**3b**), values typical of many rubbers. At an elongation higher than 10%, **3a** begins to flow irreversibly with increasing stress values. This is indicative of successive parallel alignment of the poly(diallyldimethylammonium) chains due to the mechanical field. The material can be stretched up to an elongation of 300%. At this elongation it break at a stress of 1.8−1.9 MPa. Films of **3b** break at a maximum elongation of 9% and a stress of 1.1 MPa. Because of the trisiloxane moieties, **3b** is not expected have a higher tensile modulus and a lower maximum elongation than **3a**. Obviously, in contrast to **3a**, no sliding of ionic and nonionic sheets is possible in the case of **3b**. As derived from SAXS data, the lamellar sheets of **3a** are completely smooth, which easily allows a sliding of the planes, whereas the sheets of **3b** are slightly undulated and entangled. This causes a much higher friction, resulting in a high modulus and breakage, at comparably smaller elongations. In addition to their surface energies, the high mechanical deformability makes the complexes interesting as flexible water-repellent coatings.

E. Thermal Analysis. The thermal behavior of the complexes was observed by DSC. DSC traces of complexes **3a** and **3b** show glass transitions at −10 and −56 °C, respectively. The low glass transitions explain the high flexibility of the films at room temperature. The lower glass transition of **3b** compared with **3a** is very likely due to the high flexibility of the siloxane segments of the surfactant. No further transition could be observed in the range of −100 to +200 °C. This confirms the results from WAXS, which concluded that both complexes are noncrystalline.

Table 2. X-ray Data

complex	d [nm]	b [nm^{-1}]	L [nm]	d_1 [nm]	d_2 [nm]	l_p [nm]	S/S_0
3a	2.63	0.086	2.58	1.03	1.55	1.23	1.01
3b	3.57	0.140	3.34	1.03	2.31	1.27	1.12

4. Summary and Conclusions

It has been shown that the silicon surfactants **2a** and **2b** form mesomorphic complexes **3a** and **3b** with low-energy surfaces when anchored to the polyelectrolyte **1** (Table 2). The mesophases found are lamellar smectic A-like systems, built of ionic and nonionic layers, with a long period of 2.63 nm (**3a**) and 3.57 nm (**3b**). The ionic layers of both complexes have the same thickness (1.03 nm). The nonionic layers are rich in alkyl chains and silyl groups; their thicknesses are 1.55 and 2.31 nm for **3a** and **3b**, respectively. Furthermore, both lamellar two-phase systems show sharp density transitions, representing well-defined regions of ionic and nonionic layers. The surface energy of **3b** is very much lower than that of **3a**. It is concluded that the pendant silyl groups of **3b** are oriented in a densely packed array on the surface, while those of **3a** are not packed so densely and perfectly. The lower order of **3a** is explained by packing constraints and repelling of dipole interactions in the surface layer. In contrast to that, the flexibility of the siloxane moieties of **3b** produces a molecular arrangement with lower surface energy. We conclude that for low-energy surfaces, on the basis of silicon−surfactant-containing polyelectrolyte−surfactant complexes, the length of the silicon chain has to be at least three Si atoms. For monolayers of partially fluorinated fatty acids, Zisman[23] found that uncompensated dipoles at the junction of $-CH_2-$ and CF_2- chains raise the wettabilty of monolayers if the fluorinated chain has a length smaller than seven carbon atoms.

In the future, the use of less hydrophilic polyelectrolytes will be favored. A strong hydrophilic polyelectrolyte always opposes the formation of a water-stable coating. Only little imperfections and defects in the surface cause swelling with water. It is known that cross-linking of siloxane chains at temperatures greater than 200 °C enhances the coating quality. Such annealing seems to be very promising because we have already found that the storage of fluorine complexes at 40−60 °C results in significantly enhanced surface properties. This is due to the healing of surface damages and packing faults at elevated temperatures.

Acknowledgment. The authors thank C. Remde for help during the preparation of the samples, Goldschmidt AG for providing the surfactant **2a**, and R. Wagner for help in the synthesis of **2b**. We are also grateful to M. Antonietti and C. Göltner for many helpful suggestions. Financial support was provided by the Max Planck Society.

LA980229G

(23) Shafrin, E. G.; Zisman, W. A. *J. Phys. Chem.* **1962**, *66*, 740. references.